JOURNAL OF CHEMICAL ENGINEERING AND INDUSTRIAL BIOTECHNOLOGY
E-ISSN: 0126-8139
VOLUME 11, ISSUE 2, OCTOBER 2025, 1 – 10
DOI: https://doi.org/10.15282/jceib.v11i2.12041

RESEARCH ARTICLE

Biodegradable Saponins from Fenugreek Seeds as Eco-Friendly Wax Deposition Inhibitors in Crude Oil Pipelines

Norida Ridzuan*, Jivithah Ramesh

Faculty of Chemical and Process Engineering Technology, Universiti Malaysia Pahang Al-Sultan Abdullah, Lebuh Persiaran Tun Khalil Yaakob, 26300, Kuantan, Pahang, Malaysia

ABSTRACT - Wax deposition in crude oil pipelines, caused by temperatures dropping below the wax appearance temperature (WAT), leads to paraffin build-up and blockage. While chemical inhibitors can prevent this, they are costly and harmful to the environment. This study explored biodegradable saponins extracted from fenugreek seeds as a sustainable alternative to inhibit wax deposition, improve the rheological behavior and compare it with commercial saponins. Saponin was extracted using chemical methods, producing white crystals in samples A, B, and C at different rotational speeds (150, 200, and 250 rpm), while commercial saponin was named Sample D. Characterization using Fourier Transform Infrared (FTIR), Gas Chromatography Mass Spectrometry (GC-MS), and Thermogravimetric Analysis (TGA) confirmed the presence of saponin, with Sample C showing the closest match to the commercial version. Cold finger analysis evaluated the wax deposition reduction, with Sample C achieving the highest paraffin inhibition efficiency (PIE) of 67.13% at 20°C and 350 rpm, 51.33% at 1 h, and 90.76% at 800 ppm. Sample C emerged as the most effective inhibitor, offering a promising and biodegradable alternative to conventional wax inhibitors used in pipelines. Future research should focus on scaling up the extraction process and testing it under various pipeline conditions.

ARTICLE HISTORY
Received : 18 Feb. 2025
Revised : 12 Nov. 2025
Accepted : 2 Dec. 2025
Published : 30 Dec. 2025

KEYWORDS
Fenugreek
Saponin
Wax Deposition
Wax Inhibitor
Cold Finger

1.0 INTRODUCTION

The petroleum industry plays a crucial role in meeting global energy demands, with crude oil remaining the primary energy source. The efficiency of this sector depends on a reliable fuel supply and uninterrupted crude oil transportation. A key factor in ensuring smooth operations is the integrity of crude oil pipelines, which are essential for maintaining flow assurance.

One of the major challenges in crude oil transportation is wax deposition in pipelinesc [1,2]. This issue can lead to restricted flow or even complete blockages, causing significant economic losses. Blockages alter flow characteristics, increasing energy consumption due to frictional pressure. Paraffin wax deposition occurs when crude oil cools during transportation, especially in offshore pipelines and cold regions [3]. When the temperature drops below the Wax Appearance Temperature (WAT), wax crystallizes and adheres to pipeline walls [5,6]. Several factors influence this process, including crude oil composition, temperature gradients, flow rates, and pipeline type. Effective wax control is necessary to maintain crude oil flow and minimize operating costs.

Traditionally, chemical additives have been used to prevent wax deposition. These inhibitors interfere with wax crystal formation, preventing adhesion to pipeline walls or reducing the crystal size. However, chemical inhibitors are expensive and pose environmental risks due to hazardous waste disposal. This has led to a demand for alternative, eco-friendly methods that are both effective and sustainable.

Natural surfactants, particularly plant-based ones, have emerged as promising alternatives to synthetic wax inhibitors. Various plant-derived substances have been studied for their ability to improve crude oil flow and reduce wax deposition. Examples include jatropha oil [7], pour point depressants from vegetable oil [8], glycerol-modified cashew nut shell liquid [9], and palm oil derivatives [10]. These natural substances have shown potential in mitigating wax-related issues without the harmful effects of synthetic chemicals.

Saponins, a class of natural surfactants, have been widely studied for their role in Enhanced Oil Recovery (EOR) and wax inhibition [11-13]. Their surface-active properties reduce interfacial tension between oil and water, enhancing oil mobility and preventing wax deposition. Additionally, saponins are biodegradable and non-toxic, making them a sustainable alternative to synthetic surfactants. Despite these advantages, the use of saponins in wax inhibition is still limited, particularly in terms of their efficiency over extended periods. Further research is needed to develop market-ready saponin-based wax removers.

*CORRESPONDING AUTHOR | N. RIDZUAN | ✉ norida@umpsa.edu.my

One challenge in using saponins is the limited research on their extraction methods, especially from sources like fenugreek. The efficacy of these natural surfactants depends on the extraction process, which can affect the composition and performance of the final product. Understanding the best extraction techniques is crucial to ensuring the consistency and effectiveness of natural wax inhibitors.

This study aims to address these gaps by exploring the potential of biosurfactants extracted from fenugreek as natural inhibitors of wax precipitation in crude oil pipelines. By evaluating saponins as an alternative to chemical inhibitors, this research contributes to more sustainable practices in the petroleum industry. The findings will help determine the feasibility of plant-based inhibitors for large-scale applications, potentially leading to cost savings and reduced environmental impacts. Ultimately, this study supports the global movement toward greener industrial practices by identifying viable alternatives to conventional chemical inhibitors.

2.0 MATERIALS AND METHOD

2.1 Materials

Chemicals used for extraction purposes were 95% ethanol (Merck), petroleum ether (Sigma-Aldrich), ethyl acetate (Sigma Aldrich), chloroform (Ultra-pure, HiMedia), methanol and ethanol (Merck), and acetone (LR grade, HiMedia). Crude oil samples were supplied by Petronas Refinery Kerteh, Terengganu.

2.2 Extraction of Saponin from Fenugreek

Fenugreek seeds were cleaned and dried for 2–3 day at 100°C in a hot air oven. The dried seeds were ground into a fine powder. Fenugreek powder (30 g) was mixed with 150 mL ethanol in three beakers. These solutions were stirred using an orbital shaker at 100 rpm, 150 rpm, and 200 rpm for 12 h, producing Samples A, B, and C. A commercial saponin sample was labeled as Sample D. The supernatant was filtered and heated at 50°C to evaporate the ethanol. After adding 50 mL petroleum ether, the solution was heated to extract plant lipids and fatty acids. The residues were filtered and mixed with 75 mL ethyl acetate and chloroform for deproteinization. This mixture was heated at 50°C to evaporate it and form a crude residue. The residue was dissolved in 50 mL methanol and added dropwise to acetone to form a precipitate. The precipitate was filtered and oven-dried at 110°C for 1 h to obtain white saponin crystals. The powdered saponins were collected and characterized using Fourier Transform Infrared (FTIR), Gas Chromatography Mass Spectrometry (GC-MS), and Thermogravimetric Analysis (TGA).

2.3 Characterization of Saponin

2.3.1 FTIR

FTIR Spectrometer (Brand: Thermo Fisher Scientific) was used to examine the absorbance and infrared bands. A magnification of 15 × was used to assess each sample. The Schwarzschild objective was performed using a Hyperion 3000 FTIR microscope (Bruker Optics, Inc.) with a dry air-purged midband MCT detector cooled with liquid nitrogen. The 64 scans of 4 cm-1 were combined to obtain the spectra [14].

2.3.2 GC-MS

An Agilent 7890A gas chromatograph coupled with a 5975C inert mass spectrometer was utilized to provide detailed information about the composition and structure of chemical compounds. The GC was operated with a 30-M × 0.25 mm × 0.25 μm Ultra ALLOY-5 column, a split injector at 320 °C with a 50:1 split ratio, and helium as the carrier gas at a flow rate of 1 mL/min. The oven program consisted of a 9-min isothermal period followed by heating at 20 °C/min to 320 °C, with a total run time of 2 min. The MS conditions included a quadrupole temperature of 150 °C, transfer line at 320 °C, source at 230 °C, and scan range of 33–600 amu at 2.59 scans/s. The samples were placed in 50 μL stainless steel Eco-cups with Eco-sticks. To prepare certain samples, 3 mL of 25% tetramethylammonium hydroxide (TMAH) in methanol was added to the cups

2.3.3 TGA

Simultaneous thermogravimetric and differential thermal analysis measurements were performed using a Mettler Toledo TGA/SD TA851e, with data acquisition and analysis conducted using the STARe software (version 8.10). The samples were placed in open 70 μL alumina crucibles and heated from 30 °C to 1000 °C at a rate of 20 °C/min, following a 3-minute equilibration at 30 °C to purge the furnace. Nitrogen or oxygen was used as the purge gas at a constant flow rate of 50 mL/min.

2.5 Cold Finger Analysis

The efficacy of wax inhibitors was evaluated using a cold-finger apparatus designed to simulate the inner wall of a pipeline. The crude oil was preheated to 50°C above the WAT. To begin the experiment, as illustrated in Figure 1, the crude oil was pretreated by immersion in a water bath at 50°C for 2 h. The cold finger temperature, controlled by a circulating water bath, was set between 10°C and 20°C, and the experiment duration varied between 1 and 3 h. Once the system reached the required temperature, crude oil samples containing varying concentrations of the saponin inhibitors (200, 400, 600, and 800 ppm) were introduced. The stirrer was activated and its rotational speed was set at 150, 250, 300,

and 350 rpm after reaching the target temperature. At the end of the experiment, the stirrer was deactivated, and the wax precipitate was collected, dried, scraped, and weighed to calculate the PIE, as defined in Equation (1)[5].

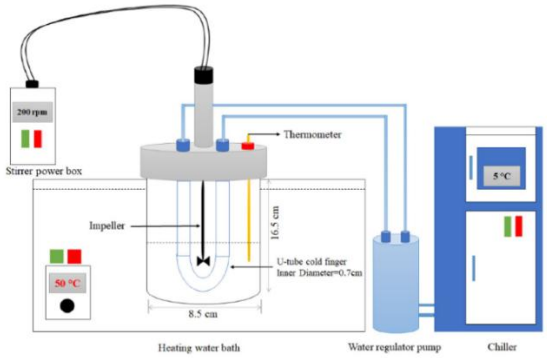

Figure 1. The cold finger apparatus.

$$PIE\ (\%) = \frac{Wf - Wt}{Wt} \times 100 \qquad (1)$$

where w_f is the reference weight of was deposition without wax inhibitor (g) and w_t is the weight of paraffin deposition with wax inhibitor (g).

3.0 RESULTS AND DISCUSSION

3.1 Profiling of Saponin Compounds

3.1.1 Functional Groups Identified in Saponins

Table 1 presents the functional groups identified in the saponins, including hydroxyl (OH), carboxyl (COOH), C-H, O-H, and C-O-O groups. These functional groups were detected in Samples A, B, and C as well as in Sample D (commercial saponin). Collectively, these groups contribute to the amphiphilic properties and biological activities of saponins [13].

Table 1.Functional group of the extracted and commercial saponin

Wavenumber (cm^{-1})				Functional Group	Range
Sample A	Sample B	Sample C	Sample D		
3352.27	3354.12	3595.47	3595.52	OH	3200-3600
1714.66	1717.20	1658.10	1641.08	COOH	1600-1725
2921.63	2850.21	2972.39	2972.38	C-H	2800-3000
1361.34	1417.86	1391.87	1394.91		1350-1450
1471.30	1438.35	1428.24	1475.54	O-H	1400-1500
1036.87	1147.69	1054.54	1054.63	C-O	1000-1200

Three samples (A, B, and C) were compared with Sample D (Commercial Saponin) using FTIR spectroscopy. The FTIR spectra of samples C and D showed considerable similarity, indicating that both share comparable functional groups and molecular structures typical of saponins (Figure 2). Notable absorption bands include broad O-H stretching bands at 3427.80 cm^{-1} for Sample C and 3387.92 cm^{-1} for Sample D, and aliphatic C-H stretching vibrations at 2924.64 cm^{-1} and 2854.10 cm^{-1} in both samples, which suggest the presence of hydroxyl and aliphatic groups. Both samples also displayed pronounced carbonyl (C=O) stretching peaks around 1736.97 cm^{-1}, confirming the presence of saponins. Additional peaks corresponding to C-O stretching and C-H bending vibrations in the 1654-1377 cm^{-1} range, as well as ether (C-O-C) and hydroxyl (C-OH) vibrations in the 1241-1034 cm^{-1} range, are consistent across both samples. The OH group exhibits a notable similarity between Sample C (1054.54 cm^{-1}) and Sample D (commercial saponin) (1054.63 cm^{-1}), as indicated in Table 1.

Although minor differences in wavenumber positions and peak intensities were observed, these variations likely resulted from slight differences in molecular composition or structural environment. Overall, the FTIR analysis suggests that Sample C closely resembles commercial saponin in terms of chemical structure and functional groups, indicating potential similarities in properties and applications.

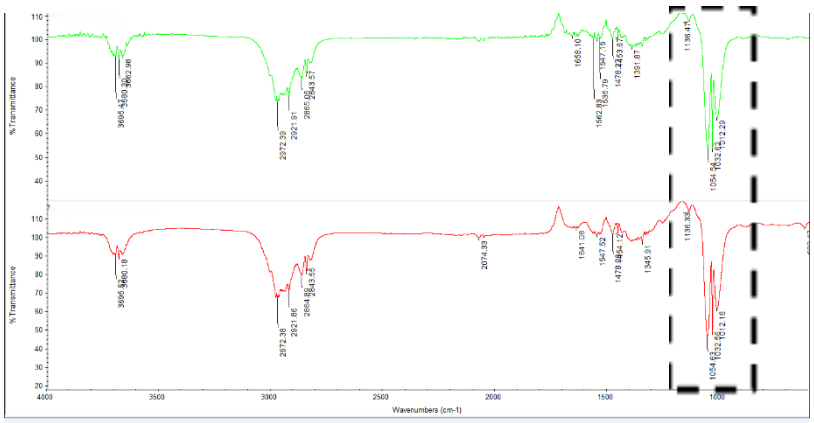

Figure 2. FTIR result of Sample C with Sample D (Commercial Saponin).

3.1.2 Peak Characteristics of Saponin Profiles Across Multiple Samples

Figure 3 presents a comparative analysis of saponin profiles across different samples, highlighting the distinct peaks and their temporal variations. In Figure 3(a), Sample A demonstrates a saponin peak at 16.981 cm^{-1} within the time range of 15 to 18 s. This peak indicated the presence of saponins with a specific wavenumber characteristic of this sample. In contrast, Figure 3(b) reveals that Sample B has a saponin peak at 16.591 cm^{-1}, reflecting a different saponin profile compared to Sample A. Further analysis in Figure 3(c) shows that Sample C exhibits a peak at 17.469 cm^{-1}. This peak is notably similar to the peak observed in Figure 4(d) for Sample D (Commercial), where the peak is located at 17.810 cm^{-1}. The proximity of these peaks suggests that samples C and D share similar saponin characteristics. From 17s to 18s, both the graphs of Sample C and Sample D (Commercial) indicate a stronger presence of the triterpenoid functional group, confirming the presence of saponin [16]. This increased intensity in the peak region corroborates the presence of saponins and highlights the commonality in the saponin profiles between these samples. The consistency in peak positioning and functional group analysis underline the significant saponin content in samples C and D, providing valuable insights into their chemical composition and potential functional properties.

3.1.3 Analysis of Saponin Stability

Examination of Figure 4, which presents the TGA data, reveals insights into the thermal properties and saponin content of Sample C compared to Sample D (commercial). The TGA curves illustrate a notable weight loss of approximately 2% (w/w) for both the samples at approximately 200°C. This initial weight loss is indicative of the elimination of volatile components, such as water or low-molecular-weight compounds, and represents the "dehydration step," which is a common feature of various chemical substances.

The thermal decomposition profiles of samples C and D (commercial) exhibited distinct behaviors as the temperature increased. At 700°C, Sample C demonstrated a higher weight retention of 39.91% than that of Sample D (Commercial), which retained 36.71%. This increased weight retention in Sample C suggests that it may possess greater thermal stability or a different compositional profile, leading to slower thermal degradation compared to Sample D (commercial). Interestingly, despite the initial expectation that Sample D (Commercial) would exhibit higher weight retention owing to its greater starting weight percentage, Sample C showed superior weight retention at 300°C. This observation implies that Sample C contains components that contribute to its enhanced heat stability or slower rate of thermal breakdown.

However, when the temperature exceeded 500°C, Sample C underwent a significant weight decrease, indicating substantial thermal decomposition. At 600°C, both the samples exhibited a marked reduction in weight, reflecting the degradation of saponins under high-temperature conditions. This thermal degradation confirms that the saponins in Sample C are stable at lower temperatures but susceptible to breakdown at elevated temperatures. Overall, the TGA results suggest that Sample C maintains a more stable saponin presence at lower temperatures than Sample D (Commercial), highlighting differences in their thermal stability and compositional characteristics.

3.2 Cold Finger Analysis

3.2.1 Effect of Temperature on the Wax Deposition

Figure 5 clearly depicts the relationship between temperature and wax formation, highlighting the reduction in wax deposits with increasing temperature. The wax formed with the extracted saponin was significantly lower than that formed with commercial saponin. Specifically, at 10°C, the wax layer deposited on the cold finger using the extracted saponin decreases from 0.67 g to 0.63 g, compared to a substantially higher deposit (1.72 g) when blank crude oil was used. This trend continues at 20°C, where the wax deposit further drops from 0.52 g to 0.47 g with the saponin, while the blank crude shows a deposit of 1.43 g.

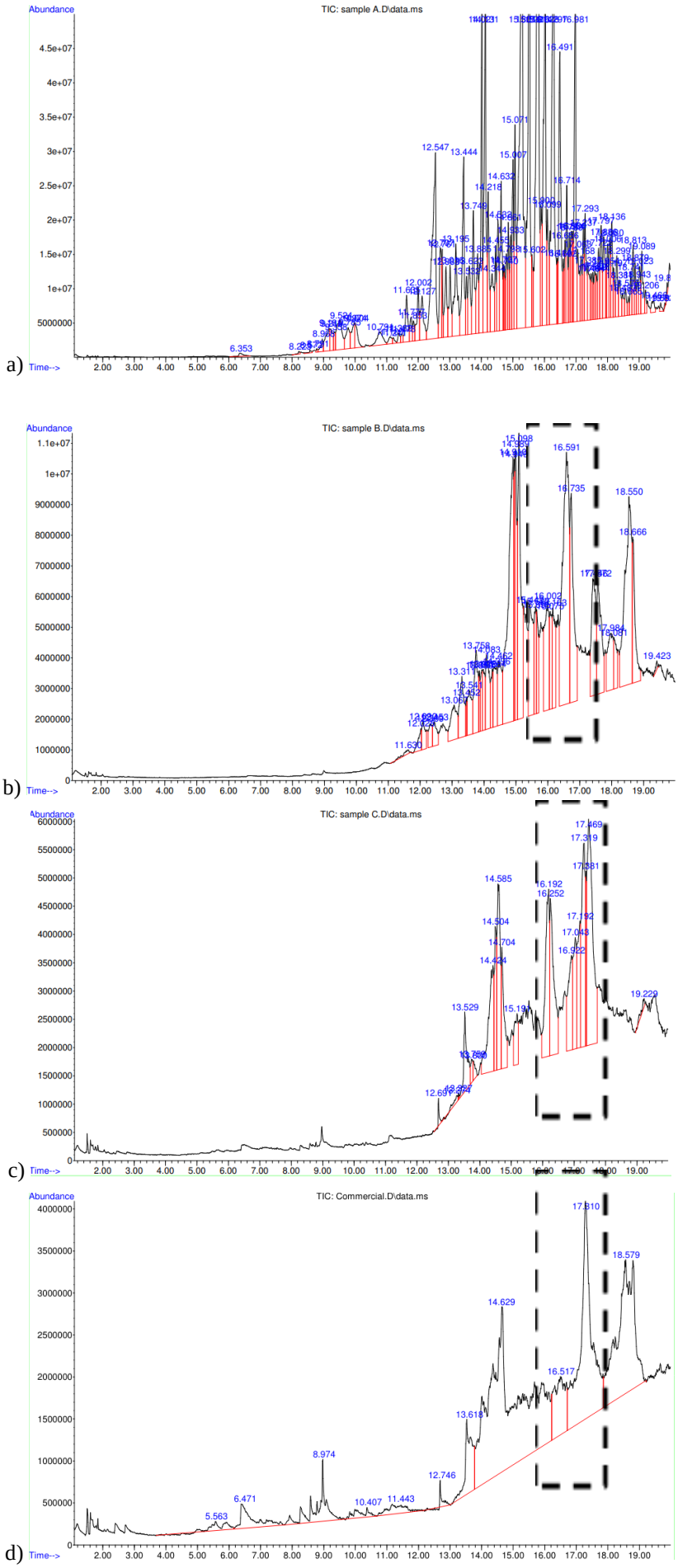

Figure 3. GC-MS Results of (a)Sample A, (b)Sample B, (c)Sample C and (d)Sample D (Commercial).

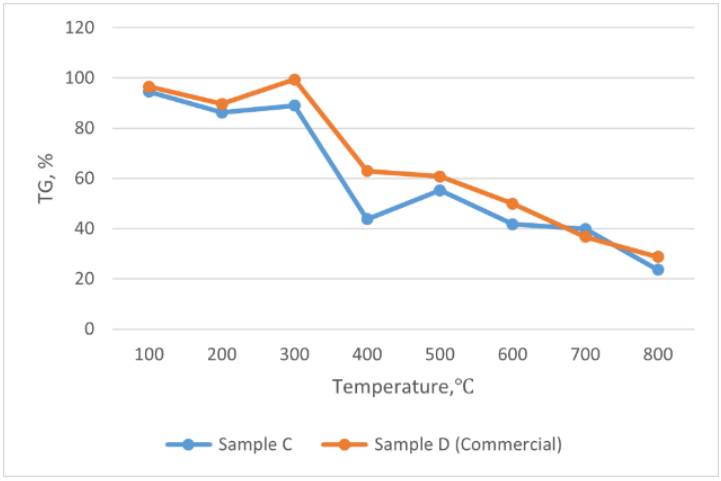

Figure 4. Comparison of TGA Sample C and Sample D (Commercial).

The reduction in wax deposition can be attributed to the improved flow characteristics of the crude oil facilitated by the presence of saponin. Higher temperatures typically enhance the fluidity of crude oil by decreasing its viscosity [14], thus reducing wax crystallization. As shown in Figure 5, at 15°C, the use of saponin resulted in the lowest viscosity, representing a 35.5% reduction. This is clearly demonstrated in the experimental results shown in Figure 6 (a), where the formation of thick and substantial wax deposits on the cold finger is attributed to the increased viscosity of 24.18 cP in the blank crude oil at 10°C. In contrast, crude oil with saponin exhibited a lower viscosity (21.84 cP at the same temperature, reducing its tendency to form wax deposits.

Figure 7 (a) to (b) further supporting this observation. Figure 7(b) illustrates the improved fluidity of crude oil at 20°C when treated with saponin compare to Figure 6(a) where the amount of wax deposit in Figure 7(b) is lesser. The viscosity of the crude oil with the saponin decreases to 10.82 cP, compared to the higher viscosity of 12.84 cP observed in the blank crude oil. This reduction in viscosity enhances the ability of oil to retain wax molecules in the solution, further minimizing wax deposition. These findings underscore the effectiveness of saponins in reducing wax formation and improving crude oil flow, particularly at lower temperatures. This improved performance is crucial for preventing operational challenges associated with wax deposition in pipelines and storage facilities.

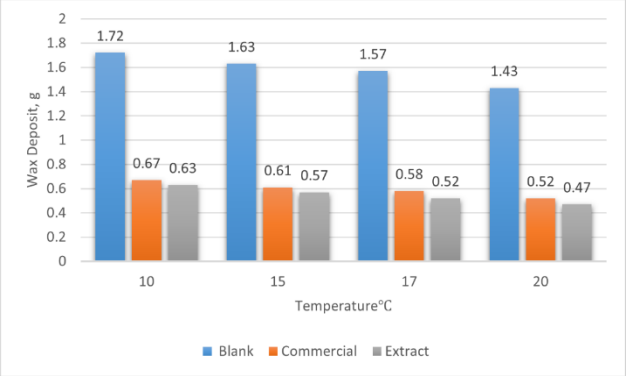

Figure 5. Effect of Temperature on the Wax Deposition.

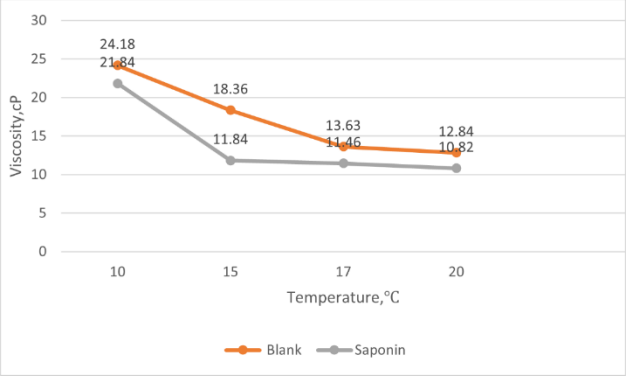

Figure 6. Effect of Temperature on the Viscosity between the Blank Crude Oil and Saponin added Crude Oil.

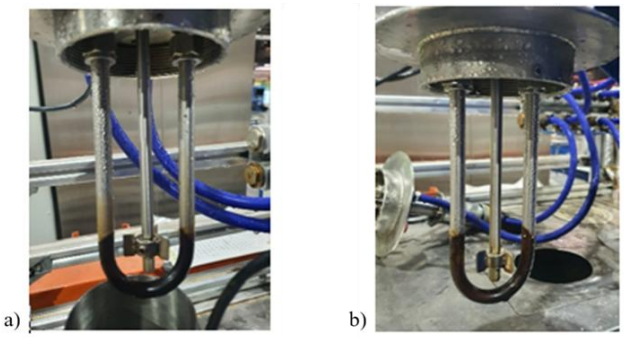

Figure 7. Wax Deposited on the Cold Finger when crude oil is added with Extracted Saponin (a)10℃ and (b) 20℃.

3.2.2 Effect of Rotational Speed on the Wax Deposition

Figure 8 shows the impact of varying rotational speeds on wax deposition in crude oil. At the lowest speed of 150 rpm, the crude oil flows in a laminar fashion, leading to a reduction in wax deposition from 1.7 g to 0.73 g, due to the slower movement and reduced shear forces [17]. As the rotational speed increased to 250 rpm, the flow became more turbulent, and wax deposition decreased further from 1.62 g to 0.66 g. At 300 rpm, the turbulence in the crude oil flow intensified, further reducing the wax formation. At the highest rotational speed of 350 rpm, the turbulence reached a peak, significantly minimizing wax deposition. The increased shear forces at this speed prevented wax molecules from settling and agglomerating.

Consequently, wax deposition is greatly reduced from 1.43 g in the blank crude oil sample to 0.59 g in the commercial saponin-treated oil, and down to 0.47 g when using the extracted saponin blend. This substantial reduction in wax deposition enhances the crude oil transport efficiency and reduces the need for additional wax mitigation strategies, maximizing the operational efficiency of the pipeline at high rotational speeds.

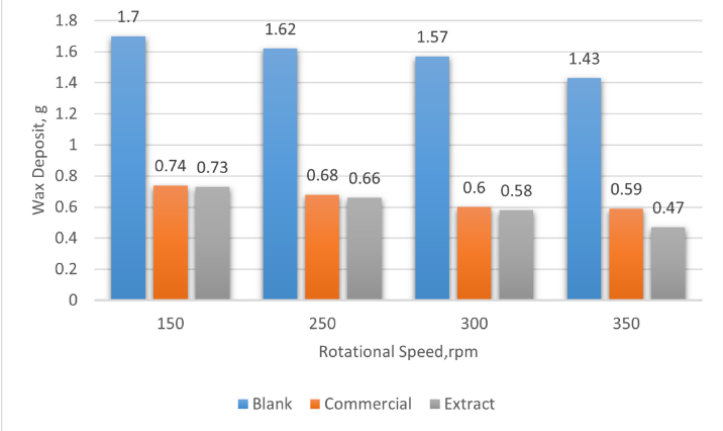

Figure 8. Effect of Rotational Speed on Wax Deposition.

3.2.3 Effect of Duration Time on the Wax Deposition

Figure 9 illustrates the progression of wax deposition over time, starting from the first hour of contact as the crude oil cools, leading to the separation of the wax molecules. After 1 h, the wax deposited measured 3 g for the blank sample, 1.53 g for the commercial saponin, and 1.46 g for the oil with the extracted saponin. As the contact time increased to 2 h, wax deposition became more pronounced owing to further heat loss from the crude oil, promoting greater wax precipitation. By 2.5 h, wax accumulation reached a more advanced stage, and the solubility of wax in crude oil decreased further with prolonged exposure to lower temperatures, resulting in increased precipitation. The extended cooling period facilitated the growth of larger wax crystals and allowed for more substantial accumulation [18]. The blank sample exhibited the highest wax deposition, with 6.07 g of wax after 3 h, followed by 5.4 g for the commercial saponin sample and 4.21 g for the extracted saponin sample.

However, as the duration of time increases, wax deposition also increases because of the continued cooling of crude oil, which further reduces its ability to hold wax in the solution. This results in more wax molecules precipitating and forming thicker and more organized deposits. Despite the overall increase in wax accumulation with extended exposure, the samples with extracted saponin showed significantly lower deposits than the blank, demonstrating better wax management even as the deposition duration lengthened.

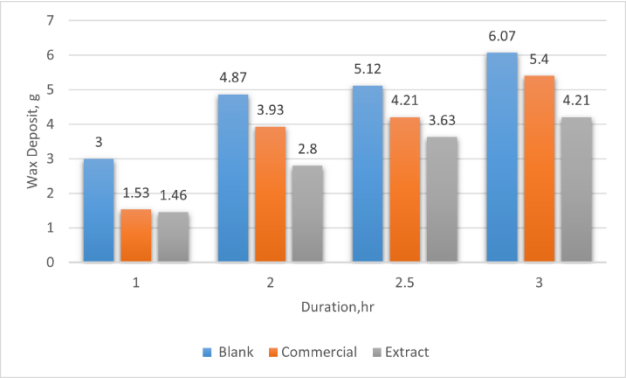

Figure 9. Effect of Duration on the Wax Deposition.

3.2.4 Effect of Inhibitor Concentration on the Wax Deposition

Figure 10 shows the influence of varying inhibitor concentrations on wax deposition, highlighting the progressive effectiveness of inhibitors as the concentrations increased. At 200 ppm, inhibitors had a minimal impact, showing a limited capacity to prevent wax deposition. However, as the concentration was increased to 400 ppm, the inhibitor efficiency improved significantly. Wax formation decreases from 2.56 g for blank crude to 0.73 g for commercial saponin and 0.64 g for extracted saponin. The interaction between wax molecules and inhibitors becomes more profound at this concentration, effectively preventing wax crystallization and reducing deposition on pipeline walls.

As the inhibitor concentration increased to 600 ppm, the efficacy in preventing wax deposition was markedly enhanced. A higher concentration allows more wax molecules to interact with the inhibitor, strongly inhibiting crystallization and further decreasing wax build-up [19]. At the maximum concentration of 800 ppm, the inhibitors provide the best defence against wax deposition, with wax formation reduced to 1.26 g for blank crude, 0.49 g for commercial saponin, and 0.46 g for extracted saponin. The inhibitors effectively prevent wax molecules from aggregating, resulting in less deposition on pipeline surfaces. In addition to wax deposition, the impact on viscosity is significant, as shown in Fig.10. The viscosity of blank crude oil, initially at 7.17 cP, is reduced to 4.57 cP with the addition of saponin at 800 ppm, indicating that higher inhibitor concentrations not only prevent wax formation but also enhance crude oil flow by reducing viscosity.

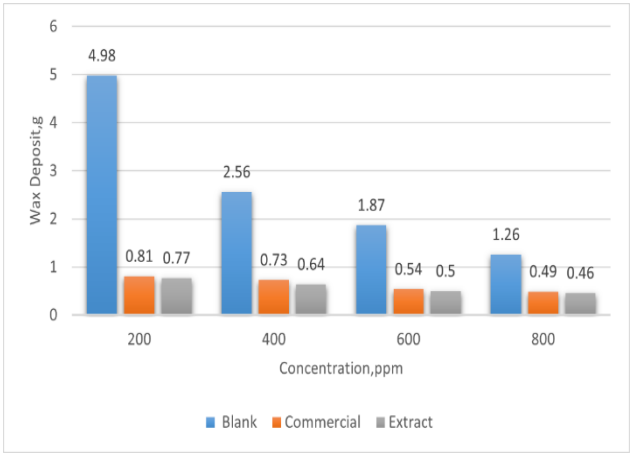

Figure 10. Effect of Concentration on the Wax Deposition.

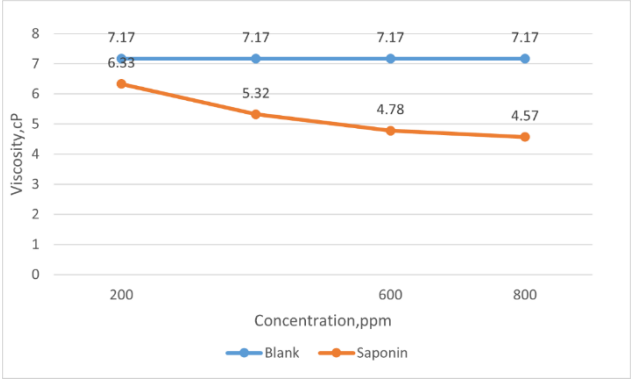

Figure 11. Effect of Concentration on the Viscosity between the Blank Crude Oil and Saponin added Crude Oil.

3.3 Analysis of Performance Inhibition Efficiency (PIE)

Tables 2, 3, 4, and 5 present the PIE of saponins under different experimental conditions. PIE was calculated using Equation 1 to evaluate the most effective factors influencing wax deposition control. According to Table 2, at a temperature of 20°C, and Table 3, at a rotational speed of 350 rpm, the highest PIE recorded was 67.13%, indicating that these parameters significantly reduce wax formation. Higher shear rates disrupt the formation of wax crystals and their adherence to pipeline walls, thereby reducing deposition [20]. When examining the effect of time (Table 4), the data showed that a duration of 1 h produced the highest PIE of 51.33%, emphasizing the importance of an early response in controlling wax deposition. Prolonged exposure times can lead to increased wax deposition; thus, optimizing the duration helps in minimizing the accumulation of wax Table 5 reveals that an inhibitor concentration of 800 ppm results in a PIE of 90.76%, making the concentration the most influential factor in wax prevention. These findings collectively suggest that the optimal conditions for achieving maximum inhibitory performance of saponin are a temperature of 20°C, rotational speed of 350 rpm, duration of 1 h, and concentration of 800 ppm. These parameters provided the most effective reduction in wax deposition, underscoring the importance of finely tuning the experimental conditions for efficient flow assurance in crude oil pipelines.

Table 2. PIE % according to the Temperature

Temperature, ℃	Weight, g(Blank)	Weight, g(Extract)	PIE, %
10	1.72	0.63	61.63
15	1.63	0.57	65.03
17	1.57	0.52	66.88
20	1.43	0.47	67.13

Table 3. PIE % according to the Rotational Speed

Rotational Speed, rpm	Weight, g(Blank)	Weight, g(Extract)	PIE, %
150	1.7	0.73	58.52
S250	1.62	0.66	59.26
300	1.57	0.58	63.06
350	1.43	0.47	67.13

Table 4. PIE % according to the Duration

Duration, h	Weight, g (Blank)	Weight, g(Extract)	PIE, %
1	3.00	1.46	51.33
2	4.87	2.8	42.51
2.5	5.12	3.63	29.10
4	6.07	4.21	30.15

Table 5. PIE % according to the Concentration

Concentration, ppm	Weight, g (Blank)	Weight, g(Extract)	PIE, %
200	4.98	0.77	84.54
400	4.98	0.54	89.16
600	4.98	0.50	89.96
800	4.98	0.46	90.76

4.0 CONCLUSIONS

This study evaluated three types of extracted saponin inhibitors against a commercial saponin to identify the optimal inhibitor to reduce wax deposits in oil pipelines. Characterization techniques, including FTIR, GC-MS, and TGA, confirmed that Sample C, obtained at 250 rpm, had the highest saponin content. Cold finger analysis showed that Sample C achieved a maximum PIE of 67.13% at 20°C, with wax deposits reduced to 0.47 g due to improved heat transfer from the impeller. At a rotational speed of 350 rpm, the maximum PIE was 67.13%. Additionally, reducing the duration decreased wax deposits from 4.21 g to 1.46 g, resulting in a PIE of 51.33%. The highest PIE (90.76 %) was recorded at a concentration of 800 ppm. The optimal conditions for performance were determined to be 20°C and 350 rpm for 1 h with 25 mL of saponin. This research highlights the potential of fenugreek-derived saponins as an effective, natural alternative to synthetic inhibitors, offering a promising pathway for improving sustainability and efficiency in the petroleum sector while supporting more environmentally friendly practices.

ACKNOWLEDGEMENTS

This study was supported by the Ministry of Higher Education (FRGS/1/2018/TK02/UMP/03/1, Grant No: RDU1901060) and Fundamental Research Grant from Universiti Malaysia Pahang Al-Sultan Abdullah (RDU230034). We also thank to Petronas Penapisan Kerteh, Malaysia for providing the crude oil samples for the research project.

REFERENCES

[1] Patel, Z., Patel, J. and Nagar, A. 2024. Role of acrylate terpolymers in flow assurance studies of crude oil. Petroleum Science and Technology 1–23. doi: 10.1080/10916466.2024.2356151

[2] Al-Shboul, T., Sagala, F. and Nassar, N.N. 2023. Role of surfactants, polymers, nanoparticles, and their combination in inhibition of wax deposition and precipitation: A review. Advances in Colloid and Interface Science 315: 102904. doi:10.1016/j.cis.2023.102904

[3] Adebiyi, F. M. 2020. Paraffin wax precipitation/deposition and mitigating measures in oil and gas industry: A review. Petroleum Science and Technology 38(21): 962–971. doi:10.1080/10916466.2020.1804400

[4] Merino-Garcia, D. and Correra, S. 2008. Cold Flow: A Review of a technology to avoid wax deposition. Petroleum Science and Technology 26(4): 446–459. doi:10.1080/10916460600809741

[5] Ridzuan, N., Adam, F. and Yaacob, Z. 2014. Molecular recognition of wax inhibitor through pour point depressant type inhibitor. Paper presented at International Petroleum Technology Conference, Kuala Lumpur, Malaysia, December 10. doi:10.2523/IPTC-17883-MS

[6] Elarbe, B., Elganidi, I. Ridzuan, N. Yusoh, K. Abdullah, N. and Vijayakumar, S. 2022. Synthesis, characterization and evaluation of stearyl acrylate-co-behenyl acrylate copolymer as a pour point depressant of waxy crude oil. Journal of Petroleum Exploration and Production Technology 12: 1811–1828. doi:10.1007/s13202-021-01408-7

[7] Akinsete., O. O. Owoseni, S. M. and Sulaimon, A. A. 2023. Experimental investigation of wax inhibition tendency of Jatropha oil in Niger Delta waxy crude-oil. Petroleum Science and Technology 42(13): 1685–1700. doi:10.1080/10916466.2022.2149800

[8] Azeem, A., Kumar, R. Pal, B. and Naiya, T. K. 2019. Use of novel pour point depressant synthesized from vegetable oil for waxy crude oil. Petroleum Science and Technology 38(3): 185–193. doi:10.1080/10916466.2019.1697291

[9] Eke, W. I., Achugasim, O. Ajienka, J. and Akaranta, O. 2020. Glycerol-modified cashew nut shell liquid as eco-friendly flow improvers for waxy crude oil. Petroleum Science and Technology 39(4): 101–114. doi:10.1080/10916466.2020.1849284

[10] Ragunathan, T., Wood, C. D. and Husin, H. 2022. Inhibiting wax deposition using palm oil additives. Journal of Petroleum Exploration and Production Technology 12(1): 99–115. doi.org/10.1007/s13202-021-01318-8.

[11] Pordel Shahri, M., Shadizadeh, S. R. and Jamialahmadi, M. 2012. A new type of surfactant for enhanced oil recovery. Petroleum Science and Technology 30(6): 585–593. doi:10.1080/10916466.2010.489093

[12] Ali, M., Chhetri, A. B. Ketata, C. and Islam, M. R. 2009. Microscopic study of oil flocculation and coalescence processes for understanding the role of surfactants in EOR performance. Petroleum Science and Technology 27(12): 1251–1260. doi:10.1080/10916460802105542

[13] Wu, Y., Wang, Y. Lei, T. and Xia, Y. 2013. The solubilization capability of polycyclic aromatic hydrocarbons enhanced by biosurfactant saponin mixed with conventional chemical surfactants. Petroleum Science and Technology 32(1): 108–115. doi:10.1080/10916466.2011.653467

[14] Almutairi, M. S. and Ali, M. 2014. Direct detection of saponins in crude extracts of soapnuts by FTIR. Natural Product Research 29(13): 1271–1275. doi:10.1080/14786419.2014.992345

[15] Ridzuan, N., Subramanie, P. and Uyop, M. F. 2020. Effect of pour point depressant (PPD) and the nanoparticles on the wax deposition, viscosity and shear stress for Malaysian crude oil. Petroleum Science and Technology 38(20): 929–935. doi:10.1080/10916466.2020.1730892

[16] Rai, S., Kafle, A., Devkota, H. P., & Bhattarai, A. (2023). Characterization of saponins from the leaves and stem bark of Jatropha curcas L. for surface-active properties. Heliyon, 9(5), e15807. https://doi.org/10.1016/j.heliyon.2023.e15807.

[17] Li, R., Huang, Q., Huo, F., Fan, K., Li, W., & Zhang, D. (2019). Effect of shear on the thickness of wax deposit under laminar flow regime. Journal of Petroleum Science and Engineering, 181, 106212. https://doi.org/10.1016/j.petrol.2019.106212.

[18] Mansourpoor, M., Azin, R., & Osfouri, S. (2019). Experimental investigation of wax deposition from waxy oil mixtures. Applied Petrochemical Research, 9(1), 77–90. https://doi.org/10.1007/s13203-019-0228-y.

[19] Magashi, T., Akintola, S. A., Ebere, F. O., Magashi, L. N., & Fulalo, L. D. (2024). Comparative analysis of the effect of plant-based and petroleum-based wax inhibition additives on heavy crude oil in the Niger-Delta. SSRN. https://doi.org/10.2139/ssrn.4935800.

[20] Ridzuan, N., Adam, F., & Yaacob, Z. (2015). Effects of shear rate and inhibitors on wax deposition of Malaysian crude oil. Oriental Journal of Chemistry, 31(4), 1999-2004. https://doi.org/10.13005/ojc/310417